THE
PHYSICAL REVIEW

A journal of experimental and theoretical physics established by E. L. Nichols in 1893

SECOND SERIES, VOL. 140, No. 6A 13 DECEMBER 1965

Determination of L Binding Energies of Krypton by the Photoelectron Method*

MANFRED O. KRAUSE
Oak Ridge National Laboratory, Oak Ridge, Tennessee
(Received 16 July 1965)

Energies of the photoelectrons Kr $L_{I,II,III}$(Mo $L\alpha$), Kr $L_{I,II}$(Mo $L\beta_1$), Kr L_I(Ag $L\alpha$), Kr L_I(Ti $K\alpha$), and Kr L_I(Cr $K\alpha$) were measured with a 90° electrostatic analyzer. Krypton was irradiated in the gaseous phase. The following values of the binding energies of krypton L electrons were obtained: $L_I = 1921.2 \pm 0.8$ eV; $L_{II} = 1727.2 \pm 0.6$ eV; $L_{III} = 1674.8 \pm 0.6$ eV. These values are compared in modified Moseley diagrams with the L binding energies of neighboring elements.

THE binding energies of krypton found in most tables are based on the work of Cauchois[1,2] and Brogren.[3] Brogren derived the L energy levels from absorption edges while Cauchois derived the L_{II} and L_{III} energy levels from the $K\alpha$ emission lines with reference to the K absorption edge.[3] In addition to these measurements Moore[4] evaluated the L_I level from the $L\beta_4$ and $L\beta_3$ lines in conjunction with the M_{II} and M_{III} levels as given by Cauchois.

Cauchois' tables list the L_{II} and L_{III} binding energies as 1726 and 1675 eV, respectively. The accuracy of these values is probably not greater than a few electron volts because of the limited accuracy of the values of the krypton $K\alpha$ x-ray energies and the difficulties in defining absorption edges. The L_I binding energy is given by Moore as 1921 eV and by Brogren as 1904 eV. The latter value is probably not very dependable because of the intricacy of associating the proper edge in the absorption spectrum with the expected low-contrast edge of the L_I level. Although Moore arrived at his value from unresolved $L\beta$ lines, it agrees well with the value that is obtained in a modified Moseley-diagram interpolation from recently measured binding energies of neighboring elements.[5,6]

The present study is aimed at establishing the L_I binding energy and possibly improving the accuracy of the values of the L_{II} and L_{III} binding energies. Binding energies are derived from the energies of the L photoelectrons that are ejected by characteristic x rays from various targets as, for instance, by Mo L and Ag L x rays.

APPARATUS AND EXPERIMENTAL

Figure 1 shows a schematic drawing of the experimental apparatus. The electrostatic analyzer consists of two spherical-sector plates with radii of 17 and 23 cm, and lateral and longitudinal angles of 35° and 90°. Entrance and exit baffles enclose a half-angle of $2\frac{1}{2}$ deg; the object aperture A is 0.25 cm in diameter. The electron source extends over approximately 0.25 cm $\times$0.9 cm under x-ray bombardment and approximately 0.25 cm $\times$ 0.2 cm under electron bombardment. A 15-stage dynode structure, EMI 9603B, serves as detector. The x-ray beam, defined by a series of baffles, enters the source volume perpendicular to the electron optical axis and is trapped by an aluminum plate which serves also as an x-ray flux monitor in conjunction with an electrometer. Voltages to the analyzer plates are derived from a modified Fluke Power Supply Model 408BDA and set by reference to a Rubicon potentiometer.

All instrument walls seen by the electrons before analysis are coated with a thin layer of carbon from an Aquadag solution. Therefore, electrons are born at the vacuum potential of the spectrometer and the work function ϕ of the surface material does not enter the energy balance $E_{\text{photo}} = h\nu - E_B$ as long as gaseous targets are used.

For calibration, experimental conditions of the measurements of the Kr L photoelectrons were sim-

* Research sponsored by the U. S. Atomic Energy Commission under contract with the Union Carbide Corporation.
[1] Y. Cauchois, J. Phys. Radium **16**, 253 (1955).
[2] Y. Cauchois and H. Hulubei, Compt. Rend. **197**, 681 (1933).
[3] G. Brogren, Nova Acta Regiae Soc. Sci. Upsaliensis **14**, No. 4 (1948).
[4] H. R. Moore, Proc. Phys. Soc. (London) **A70**, 466 (1957).
[5] I. Anderson and S. Hagström, Arkiv. Fysik **27**, 161 (1964).
[6] A. Fahlman, O. Hörnfeldt, and C. Nordling, Arkiv Fysik **23**, 75 (1962).

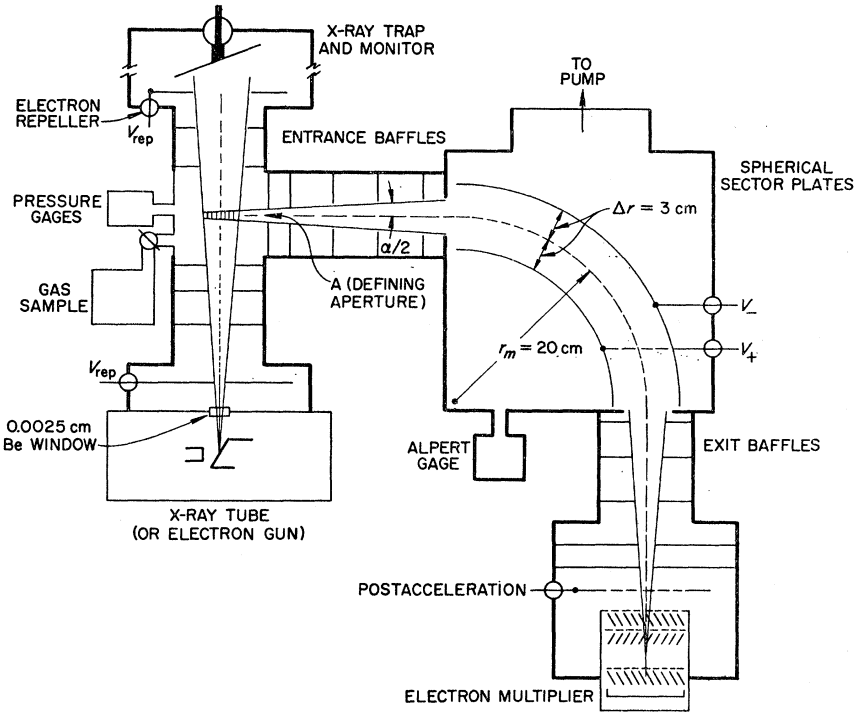

FIG. 1. Schematic diagram of electrostatic energy analyzer and electron source.

ulated by using photoelectrons of well-known energies from gaseous sources. Then, the work function ϕ could be eliminated in the following relation between the energy of the electrons E and the voltage V applied to the analyzer plates:

$$E-\phi=fV=250\ fR,$$

where R=potentiometer reading, $V/R=250.00$ and f=conversion or calibration factor.

With $\phi=0$, a single determination would suffice to base the calibration on one x-ray line and one energy level. Two determinations with a common energy level would allow basing the calibration on two x-ray reference lines. Inasmuch as the factor f proved energy-dependent, because of magnetic fields penetrating the shields, a number of photolines were necessary over an extended range of energies for calibrating the instrument. The chosen photoelectron lines are listed in the lower part of Fig. 2. Energies of x-ray reference lines are listed in Table I and binding energies of the M_{III}, M_{IV}, and M_V electrons of mercury are reported[7] as 2847.0, 2384.8, and 2294.9 eV, respectively, with an uncertainty of ±0.4 to $+0.5$ eV. The binding energy of the K electron of argon is given[8] as 3203 eV with an uncertainty of about ±1 eV. Uncertainties of the reference levels and lines were not included in the error bars of the calibration points. The shown errors, typically $\pm0.1\%$, reflect the uncertainty of positioning the peaks and the unlinearity of the potentiometer.

TABLE I. Energies of x rays used for calibration and experiment. Values calculated with $E\lambda_s=12\,372.53$ keV xu.

Line	Energy[a] (eV)	Relative intensity[a]	Peak value (eV)
Cr $K\alpha_1$	5414.7	100	5411.6
Cr $K\alpha_2$	5405.5	50	
Cr $K\beta_{1,3}$	5946.6		
Ti $K\alpha_1$	4510.8	100	4508.8
Ti $K\alpha_2$	4504.8	50	
Ti $K\beta_{1,3}$	4931.8		
Ag $L\alpha_1$	2984.4	100	2983.8
Ag $L\alpha_2$	2978.3	9	
Ag $L\beta_1$	3151.0		
Mo $L\alpha_1$	2293.2	100	2292.8
Mo $L\alpha_2$	2289.9	13	
Mo $L\beta_1$	2394.8		

[a] According to A. E. Sandström, Ref. 8, pp. 237, 177–181.

Figure 2 also shows the "difference line" AlK (Cr $K\beta$—Cr $K\alpha$), whose energy is independent of the values of the Al K level and ϕ. In addition to the above internal calibration, an external calibration was performed by means of elastically scattered thermionic electrons. The unidentified points in Fig. 2 correspond to this energy calibration. The estimated uncertainty in the energy of the electrons which amounted to the major part of the error was included in the error bars.

The calibration remained constant during the course of the measurements. In particular, no evidence was found for *local* changes in surface potentials caused by adsorbed gases or other causes which could have influenced the position of the peaks.

[7] A. Fahlman and S. Hagström, Arkiv Fysik **27**, 69 (1964).
[8] A. E. Sandström, in *Handbuch der Physik*, edited by S. Flügge, Berlin-Göttingen-Heidelberg (Springer-Verlag, Berlin, 1957), Vol. XXX, p. 215.

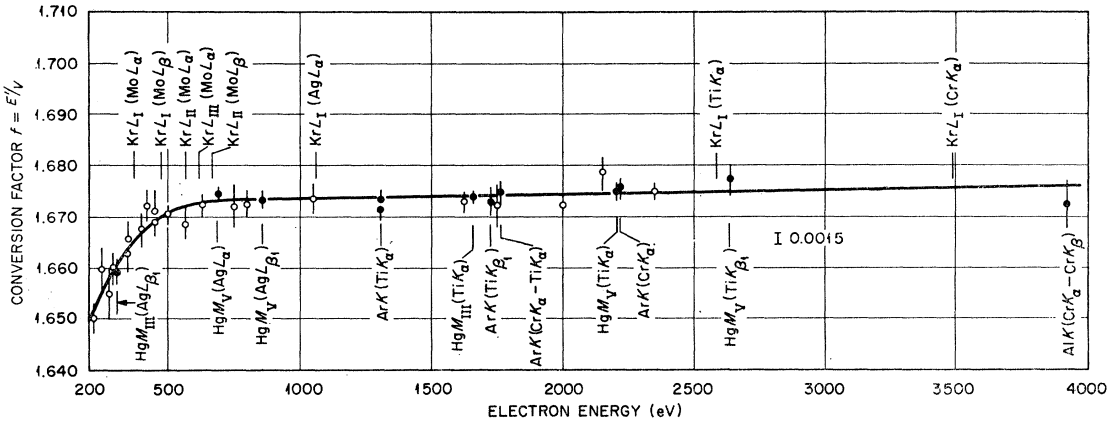

FIG. 2. Dependence of conversion factor f on electron energy $E'=E-\phi$. The calculated value is $f=1.671$. Designated points were obtained from photoelectron lines, unidentified points from elastically scattered electrons.

The resolution of the spectrometer was determined to $(2.5\pm0.1)\%$ for a source resembling a point source and $(2.7\pm0.1)\%$ for an extended source as encountered in the experiment.[9] Resolution and peak shape were independent of energy.

Krypton was introduced into the source volume at a pressure[9] of about 9×10^{-4} Torr. The partial pressure of the residual gas was less than 8×10^{-6} Torr in the source volume. Analyzer and detector sections were kept at a pressure of about 5×10^{-6} Torr by means of strong differential pumping. The path of electrons at the higher pressure in the source volume was 1 to 2 cm, so that only a small fraction of the electrons was scattered. X rays consisted of characteristic lines and bremsstrahlung from Cr, Ti, Ag, and Mo anodes. Machlett 50AEG tubes were used for Cr and Ti radiation, and a specially designed tube for Ag and Mo x rays. The Mo and Ag targets were cleaned periodically to remove tungsten deposits, which caused a drop of about 5% in the intensity of the Mo L and Ag L lines over a period of 20 h. Counting times of 8 to 15 h were required for each peak because of the low counting rates[9] of 6 to 12 counts per min (peak values) and the unfavorable signal-to-noise ratio of the detector system ranging from 0.4 to 1.8. Data points were taken alternately on either flank of the peak. Photoelectrons with less than 600 eV energy were postaccelerated by 150 to 350 V to increase the secondary electron yield of the first dynode of the electron multiplier.

During the experiment fluctuations of the sample gas pressure amounted to 2%, those of the x-ray tube voltage and x-ray flux to about 2 and 3%, respectively. The pressure drop was less than 3% per hour and the drop of the Mo L-line intensities was about 0.2% per hour. Data were corrected for drifts. This correction, however, was always smaller than the counting statistical standard deviation. Voltages to the analyzer plates could be reproduced within 0.02 to 0.04% and the symmetry of the negative and positive voltage was better than 0.04%. The linearity of the Rubicon potentiometer was checked with a K potentiometer and proved to be 0.02 to 0.03%, depending upon the range.

RESULTS AND DISCUSSION

Figure 3 shows the photoelectron peaks Kr $L_{I,II,III}$ (Mo $L\alpha$) after subtraction of the counter background. The ordinate is not corrected for the variation of window width of the spectrometer. The position of the peak is determined by lines drawn through the midpoints of parallel chords. Error bars of the data points correspond essentially to the errors in counting statistics. Asymmetry of the peaks is small and does not affect the determination of the line position.[10] The area between the broken lines and the solid lines shows the contribution of the scattered electrons to the undisturbed peak. Each peak consists of two unresolved lines that correspond to the incident $L\alpha_1$ and $L\alpha_2$ x rays. Instead of separating the lines graphically, the x-ray energy corresponding to the peak value of the composite peak was calculated from $L\alpha_1$ and $L\alpha_2$ energies and the intensity ratio of $L\alpha_1:L\alpha_2=100:13$ for molybdenum and a ratio of 100:9 for silver. Table I summarizes the energies of the peak values that were obtained from the line values given by Sandström.[8]

Primary data, photoelectron energies and binding energies of the L_I, L_{II}, and L_{III} levels are listed in

[9] At a later stage of the work, the resolution was improved to 2%. Also it was found that the pressure in the source volume could be increased to 10^{-2} Torr without shifting the peak noticeably. The low-energy tail increased, however. A pressure of less than 3×10^{-5} Torr was maintained in the analyzer section. With an 8–10-times increased counting rate and with the selection of a low-noise electron multiplier the signal-to-noise ratio was improved by a factor of 20 to 30 over the former arrangement. In Table II the superscript e designates those peaks that were measured under these conditions.

[10] The ambiguity of drawing the peak contour was reduced by knowing the peak shape. For the purpose of determining the contour, the peak was scanned by applying a repetitive sawtooth to the analyzer plates. Signals corresponding to small voltage intervals were then stored in a pulse-height analyzer operated as a multiscaler. Any fluctuations and drifts of pressure and x-ray flux were immaterial in this mode of operation.

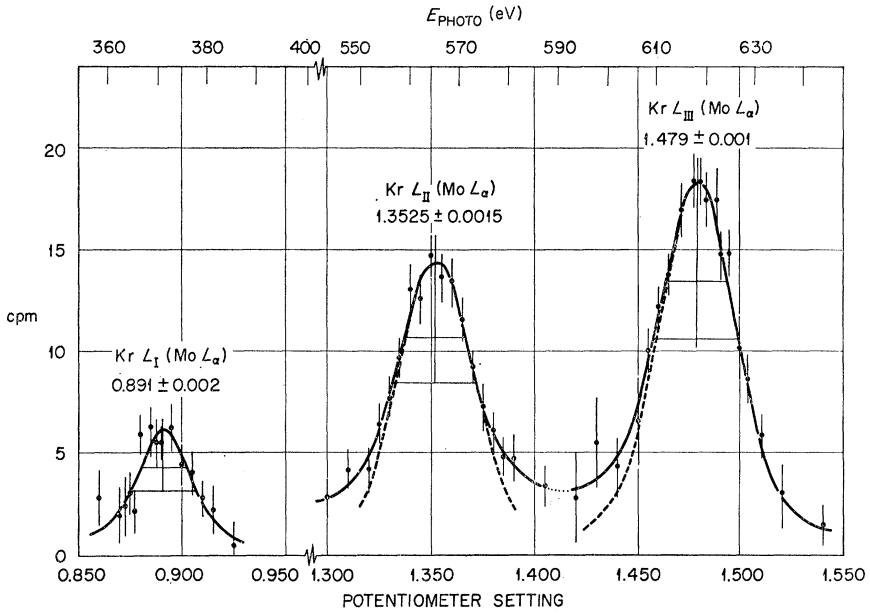

FIG. 3. Peaks of krypton L electrons ejected by Mo $L\alpha$ x rays. (Mo $L\alpha$=2292.8 eV) cpm=counts per min.

Table II. Errors assigned to the potentiometer readings of the line positions are estimated and amount to about 5% of the half-width of the peak. Values of the conversion factor f are taken from the curve in Fig. 2 at the indicated positions. The given errors allow for the choice of drawing the curve. It is, as a systematic error, added quadratically to the weighted mean error after averaging. The final binding energies represent a weighted average according to the errors of the individual determinations. As shown in Table II, relative errors in peak position and conversion factor amount to about ±0.1% each for all photoelectron lines, except for the Kr L_I (Mo L) lines, which positions are ascertained with an accuracy of about ±0.25%. No error is assigned either to the energy values of the x-ray lines or to the calculated peak values of the $L\alpha$ and $K\alpha$ doublets. The calculated $L\alpha$ values can shift by about 0.1 eV with smaller changes in the intensity ratios of the $L\alpha_1$ and $L\alpha_2$ lines.

In Fig. 4 the krypton binding energies are plotted in modified Moseley diagrams together with binding energies of the adjacent elements[5,6] previously obtained by the photoelectron method. X-ray determinations according to Sandström[8] have been used for some levels of elements between Ge and Se. With terms in Z^4 included in this representation,[11] straight lines can be drawn through the points of $Z=37$ to 39 and $Z=32$ to 35. Points belonging to krypton clearly lie close to the extended branch of the lines through $Z=37$ to 39. Breaks in the diagrams occur at $Z=35$ before the $4p$

TABLE II. Spectrometer data, energies of photoelectrons, and L binding energies (BE) of krypton.

Photoline	Potentiometer R	Conversion factor f	E_{photo} (eV)	σ_1[a] (eV)	σ_2[b] (eV)	BE (eV)	(BE) (av.)[c] (eV)
L_I (Cr $K\alpha$)	8.334 ±0.007	1.6771±0.0015[d]	3494.2	3	3	1917.4	
L_I (Ti $K\alpha$)	6.170 ±0.005	1.6765±0.001[d]	2586.0	2.1	1.9	1922.8	L_I:
L_I (Ag $L\alpha$)	2.541 ±0.004	1.6748±0.001[d]	1063.9[e]	1.6	0.7	1919.9	1921.2±0.8
L_I (Mo $L\beta_1$)	1.135 ±0.003	1.6700±0.002	473.9	1.2	0.6	1920.9	
L_I (Mo $L\alpha$)	0.891 ±0.002	1.6653±0.002	370.9	0.8	0.5	1921.9	
L_{II} (Mo $L\alpha$)	1.3525±0.0015	1.6722±0.0015	565.4	0.6		1727.4	L_{II}:
	1.3530±0.0015		565.6	0.6	0.5	1727.2	1727.2±0.6
	1.353 ±0.002		565.6[e]	0.8		1727.2	
L_{II} (Mo $L\beta_1$)	1.5965±0.0025	1.6732±0.001	667.8[e]	1.0	0.5	1727.0	
L_{III} (Mo $L\alpha$)	1.4770±0.0015	1.6726±0.001	617.6	0.6		1675.2	
	1.478 ±0.003		618.0	1.2	0.5	1674.8	L_{III}:
	1.4790±0.0015		618.4	0.6		1674.4	1674.8±0.6
	1.4775±0.0015		617.9[e]	0.6		1674.9	

[a] Error in determining peak position.
[b] Error due to uncertainty of conversion factor f.
[c] Weighted averages and weighted errors.
[d] Values greater than obtained from Fig. 2 because of scale factor of 1.0008.
[e] See Ref. 9.

[11] S. Hagström, Z. Physik **178**, 82 (1964). S. Idei, Rept. Tohuku Univ. **191**, 641 (1930).

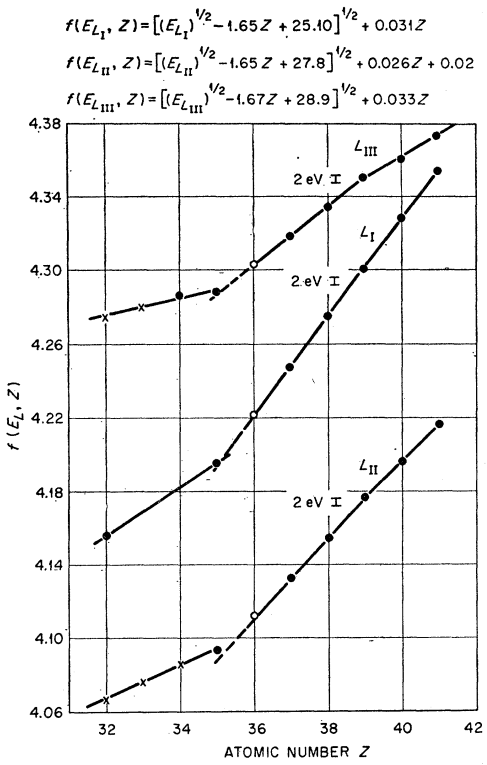

FIG. 4. Modified Moseley diagrams of the L_I, L_{II}, and L_{III} levels for $Z=32$ to 41. Points represent photoelectron data, crosses represent x-ray data, open circles show present measurements.

shell is completely filled. This is analogous to a break in the K-level diagram at $Z=17$ before the $3p$ shell is filled.[12] It was reported earlier[6] that the difference of the square roots of the L_I and L_{II} levels varies linearly with Z, as shown in Fig. 5 for $Z=35$ to 42. The present data on krypton fit well into this representation, indicating the present term difference L_I–L_{II} of krypton compares excellently with the analogous term differences of the adjacent elements. However, the point, calculated with the interpolated binding energies (Fig. 4), lies above the line by about 1 eV.

The energy of the spin doublet splitting L_{II}–L_{III} can be calculated satisfactorily with Sommerfeld's formula and it has been shown that good agreement

[12] S. Hagström and S. Karlsson, Arkiv Fysik **26**, 451 (1964).

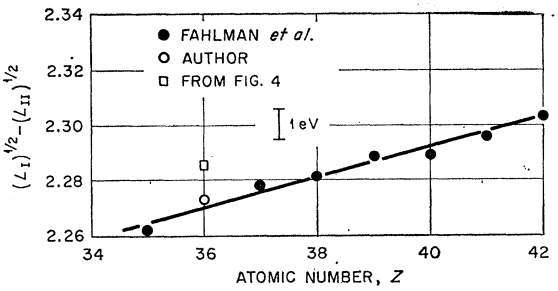

FIG. 5. Z dependence of $(L_I)^{1/2}$–$(L_{II})^{1/2}$ in the range $Z=35$ to 42. Energies are determined by the photoelectron method. No points are given for $Z=33$ and 34, since the L_I levels have not been measured for these elements.

with experimental values[6] can be obtained with a screening parameter of $d=3.50$ for the elements $Z=38$ to 47. With the same value a splitting of 52.3 eV is calculated for krypton which compares well with the experimental value of 52.4±0.5 eV.

Table III lists the L_I, L_{II}, and L_{III} binding energies of krypton quoted in various tables, Moore's value for L_I and the present measurements together with the interpolated values according to Fig. 4. While the

TABLE III. Binding energies (in eV) of the L electrons according to various sources.

	HB[a]	*C*[b]	*M*[c]	*FH*[d]	*MD*[e]	Author
L_I	1904	1904	1921	1931	1921	1921.2±0.8
L_{II}	1729.6	1726		1727	1726	1727.2±0.6
L_{III}	1677	1675		1675	1675	1674.8±0.6

[a] A. E. Sandström, Ref. 8, p. 215; see also G. Brogren, Ref. 3.
[b] Y. Cauchois, Ref. 1.
[c] H. R. Moore, Ref. 4.
[d] S. Fine and C. F. Hendee, Nucleonics **13**, 36 (1955), data obtained by least-squares interpolation in Moseley diagram from data prior to 1955.
[e] Interpolated in modified Moseley diagram with binding energies obtained by the photoelectron method. Reference 5 for Br and Rb; Ref. 6 for Sr to Pd.

previous less accurate evaluation of the L_{III} binding energy from x-ray data and the interpolated value are in accord with the present determination, the respective evaluation of the L_{II} binding energy is found to be too low by about 1 eV. The L_I binding energy of 1921 eV of the present photoelectron determination shows the correctness of Moore's previous preliminary evaluation from $L\beta$ x-ray energies.